# Numerical estimation of pressure drop of subcooled parahydrogen flow in the ESS Cryogenic Moderator System

**Vivek Sharma[1], Gen Ariyoshi[2], John G. Weisend II[3], Parthasarathi Ghosh[1] and Hideki Tatsumoto[3]**

[1]Indian Institute of Technology Kharagpur, West Bengal, India
[2]J-PARC, Japan Atomic Energy Agency, Tokai, 319-1106, Japan
[3]European Spallation Source (ESS) ERIC, Partikelgatan 2, Lund, Sweden

hideki.tatsumoto@ess.eu

**Abstract**. The Cryogenic Moderator System (CMS) at the European Spallation Source (ESS) is designed to supply liquid hydrogen at 17.5 K and 1.0 MPa to moderators for efficient neutron moderation. The liquid hydrogen is circulated with the help of a series of two pumps through CMS loop with various components, including as straight pipes, bends, reducers, corrugated pipes heat exchangers and valves etc. To optimize the CMS operational conditions, it is essential to understand the temperature and pressure propagation behaviours across the CMS. The ESS is developing a one-dimensional simulation code to predict the time-dependent temperature propagation across the CMS. In the model, the circulation flow rate is determined from the pump performance characteristics and the pressure drop. In this study pressure drops across each component were estimated using computational fluid dynamics (CFD) simulations with Ansys FLUENT. Pressure drop correlations were then derived from based on the simulation data. It was demonstrated that the predicted pressure drops could be expressed within 13% deviation, compared with the pressure drop obtained in the preliminary CMS commissioning using helium.

## 1. Introduction

The European Spallation Source (ESS) is a research facility that is designed to produce high-brightness, long-pulsed cold and thermal neutron fluxes through the spallation process. At ESS, a 5-MW proton beam strikes a tungsten target, producing high-energy neutrons [1]. These neutrons are moderated to cold energies through a light water pre-moderator and two hydrogen moderators (to be increased to four in the future), located above the target wheel, where the nuclear heating is estimated to be 6.7 kW [2].

The Cryogenic Moderator System (CMS) is designed to continuously supply subcooled liquid hydrogen at 17.5 K and 1.0 MPa. It comprises of two centrifugal pumps in series, a pressure control buffer (PCB) and an ortho-parahydrogen converter (o-p C) in bypasses, two types of heat exchangers (HXs)—a plate-fin type (HX-61100) and a finned tube type (HX-61200), cryogenic hydrogen transfer lines (HTLs), a distribution box (DB), and an in-situ o-p measurement system (OPMS) in the DB as represented in Figure 1.

Content from this work may be used under the terms of the Creative Commons Attribution 4.0 licence. Any further distribution of this work must maintain attribution to the author(s) and the title of the work, journal citation and DOI.
Published under licence by IOP Publishing Ltd

The CMS would ensure efficient moderation by supplying the liquid hydrogen flow rate of 0.5 kg/s for two moderators and 1 kg/s for four moderators [3]. The necessary circulation rates are maintained with the help of pumps, based on the pump characteristics curves that represent pressure head vs flow rate for different speeds. Therefore, accurately estimating the pressure drop across each component becomes crucial for optimizing the CMS operational conditions and ensuring the stable performance of the CMS.

For formulating such predictive, yet reliable code, precise estimation of pressure drops across each component is crucial to estimate the circulation flow rate. In this study, Computational Fluid Dynamics (CFD) simulations were carried out using Ansys FLUENT to evaluate the pressure drop across individual component as there doesn't exist direct analytical solutions for turbulent flow. The empirical correlations available for certain components are limited in their range of applicability, whereas for other components, no such correlations are available. Pressure drop correlations for each component were therefore, derived based on the simulation results. Correlations were then, compiled in the form of a simulation code for CMS. The pressure drop calculated using the code (for He) was compared with the pressure drop measured during the preliminary CMS commissioning without connecting the moderators using helium. The pressure drop estimation was, however confined to the main loop to reduce the complexity for this study.

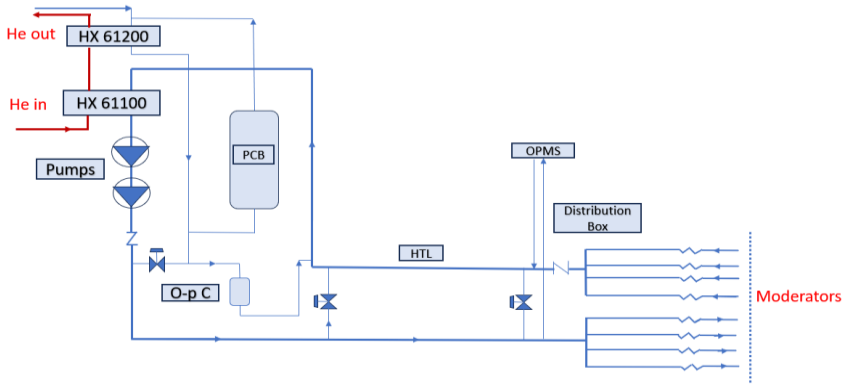


**Figure 1** Layout of Cryogenic Moderator System at ESS.

## 2. Simulation model and procedure

*2.1 Simulation model*

To accurately estimate the pressure drops across the components of the CMS, CFD simulations were performed.

The piping of the CMS consists of three different-sized pipes, DN25, DN32, and DN50 with inner diameter of 29.4 mm, 38.4 mm and 56.3 mm respectively. The 45° and 90° bends, corrugated pipes, reducers, etc., are considered as a piping component.

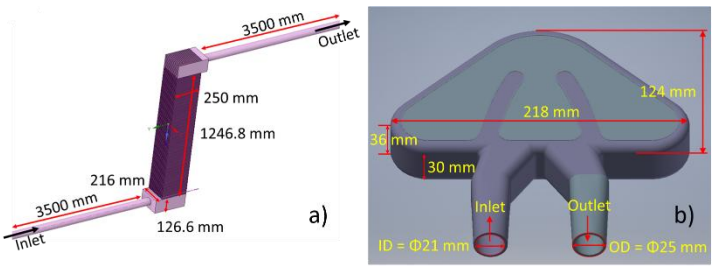


**Figure 2** Model of a) Plate-fin Heat exchanger b) Moderator

The complex shaped components can't be estimated without using a CFD analysis. The pressure drops for the HX and moderator were estimated using a CFD. The models developed for HX and Moderator are shown in Figure 2(a) and 2(b) respectively. The plate-fin type cross-counter flow HX with 29 layers is used. This 1.5 m tall HX with Liquid hydrogen ($LH_2$) flowing through 15 layers is cooled by cold incoming helium from the cryoplant. Only half of the model is considered for HX because it can be regarded as a symmetric problem. The 30 mm-thick butterfly-shaped moderator with a single vessel is adopted. The full model is applied for the moderator. A pipe with a length of 3.5 m was added to the inlet and outlet of the moderator.

In this study, the pressure drops for the piping components were also estimated using the CFD calculation.

*2.2 Simulation procedure*

The SST k−ω turbulence model is employed to accurately capture near wall flow, seperated flow and to remove dependency on wall functions for the intricate geometries. An adaptive polyhedral mesh of 3 mm size, with prism cells at boundary layer was adopted to reduce the computational time. The governing conservation equations are solved implicitly using the finite volume method. Momentum and turbulence equations are discretized using the second-order upwind scheme to ensure higher accuracy. Pressure-velocity coupling is handled through the coupled algorithm. A roughness of 0.05 mm at walls was considered. Steady-state calculations are carried out until the residual errors fall below $10^{-6}$, ensuring numerical convergence. The thermophysical properties of hydrogen at specific states are evaluated using REFPROP and the simulations were conducted for different flow rates to account for the variability in system performance.

## 3. Methodology for pressure drop estimation in Complex geometries

When estimating pressure drop from the calculated pressure distribution, it is essential to eliminate the entry length effect to ensure accurate characterization. In this study, the length of the pipe affected by the entry length effect in a straight pipe was estimated by comparing the pressure drop with the value predicted using the Colebrook equation. Figure 3(a) shows the simulation model of the straight pipe. Pipes with diameters ($D$) of 29.4 mm, 38.4 mm, and 56.3 mm were used, each with a length ($L$) of 5.0 m. Inlet and pressure boundary conditions were applied to the respective ends of the pipe. Liquid hydrogen at 17.5 K and 1.0 MPa flows with inlet flow velocities corresponding to Reynolds number ($Re$) ranging from $5\times 10^3$ to $1\times 10^6$. The velocity distribution along the center axis and pressure-gradient ($dP/dL$) calculated for DN 32 pipe with $Re = 10^5$, are presented as shown in Figure 3(b). The velocity and pressure gradient became uniform in the region where the velocity and $dP/dL$ approached constant values ($Uss$ and $Pss$). The length where the velocity reached $Uss$ was defined as $L_v$ (velocity-based entrance length). Similarly, the length at which the $dP/dL$ reached $Pss$ and

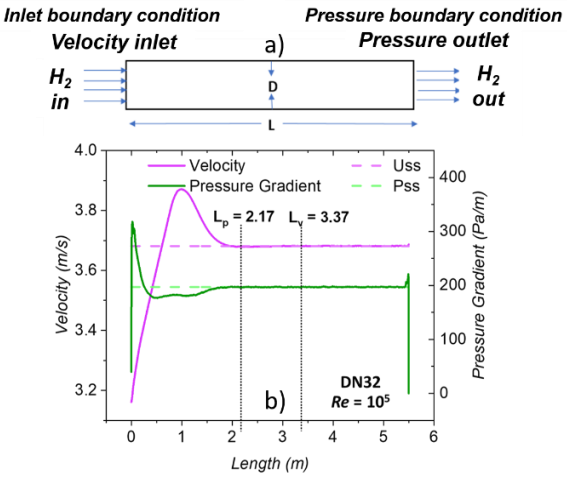


**Figure 3 a)** Simulation Model of Pipe. **b)** *Pr.-Gr.* & velocity distribution along axis of 5 m long pipe.

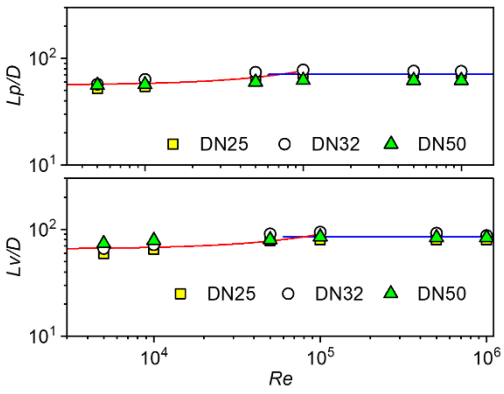


**Figure 4** Variation of $L_p$ and $L_v$ with *Re*.

aligned with the *dP/dL* distribution was defined as $L_p$ (*dP/dL*-based entrance length). The results showed that $L_v$ =3.368 m, which is longer than $L_p$ =2.172 m. As the primary objective of this study is to estimate the pressure drop, the *dP/dL*-based entrance length was adopted to avoid entry effects. Figure 4 shows the variation of $L_v$ and $L_p$ with the Reynolds number. Regardless of the pipe size, the values of $L_p/D$ and $L_v/D$ were consistent at each *Re* (For all the components, *Re* has been calculated based on the inlet pipe diameter and velocity). As *Re* increased, both values also increased; However, they became constant for $Re > 10^5$. The values of $L_v/D$ were higher than those of $L_p/D$ across the entire range of *Re*. For the largest diameter of 56.3 mm, the maximum hydrodynamic development length ($L_p$) was approximately 3 m. To account for inlet and exit effects with a safety margin, 3.5 m of straight pipe was added to both the inlet and outlet of each component.

In this study, an effective method for estimating the pressure drop across complex components was developed by combining them with inlet and outlet straight pipe sections. As a specific example, Figure 5 presents a pressure distribution for a DN50 sized bend with 3.5 m straight pipe sections on both ends. For comparison, the pressure drops in the inlet and outlet pipes calculated using the Colebrook equation are also shown in the figure. As described above, the deviations from the Colebrook equation are observed in the inlet and outlet straight pipe sections at their entrances. In the design of the cryogenic system, the total pressure drop across the loop was estimated by a linear combination of the individual pressure drops from each component. At the boundary between the component and the outlet straight section (point b), the pressure ($P_b$) was defined by extrapolating the pressure curve from the outlet straight pipe section, as calculated using the pressure gradient (*Pss*). Meanwhile, at the boundary between the inlet straight pipe section and component (point a), the pressure distribution downstream of *Uss* ($P_a$) obtained from the CFD and Colebrook equation is the same. The pressure drop ($\Delta P$) across the component was defined as $P_a - P_b$.

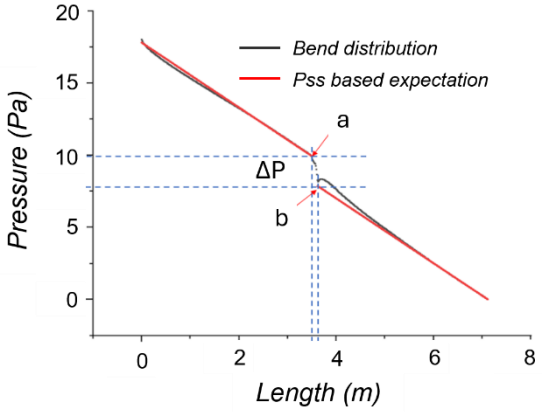


**Figure 5** Estimation of pressure drop in 90° bend at $Re = 10^5$.

## 4. Results and Discussions

### *4.1 90° and 45° bends*

Both 90° and 45° bends for *D* = 29.4 mm, 38.4 mm and 56.3 mm were simulated under the conditions where liquid and gaseous hydrogen flowed at temperatures ranging from 17.5 K to 100 K and a pressure of 1.0 MPa, with *Re* ranging from $5 \times 10^3$ to $1 \times 10^6$. Pressure drops were estimated using the defined methodology mentioned in section 3. Figures 6(a) and 6(b) show the

effect of *Re* and *D* on the pressure drop for the 90° and 45° bends, respectively, at 17.5 K. It was observed that the pressure drop with *Re* followed power law relationship (as shown by fiiting curves in Figures 6(a) and 6(b)) for all pipe sizes and decreased with increase in the pipe diameter. The pressure drops for the 90° bend were higher than those for 45° bends, although overall trend remained the same. Based on the simulation results and Darcy's equation, the following correlation was derived by introducing the bending piping length ($L$) and an empirical exponent ($\alpha$) for the length-to-diameter ratio ($L/D$).

$$\Delta P = f\left(\frac{L}{D}\right)^{\alpha}\frac{\rho u^2}{2} \tag{1}$$

$$\text{where, } \begin{cases} \alpha = 1 \\ f = 2.4Re^{-0.235} & Re < 3.25\times10^4 \\ f = 0.2055 & Re \geq 3.25\times10^4 \end{cases}$$

$$L = 2\pi R\frac{B}{360} \tag{2}$$

where $\rho$ is the density, $u$ is the velocity, $f$ is the friction factor, $R$ is the curvature radius of the bend, $B$ is the bending angle of 90° or 45°.

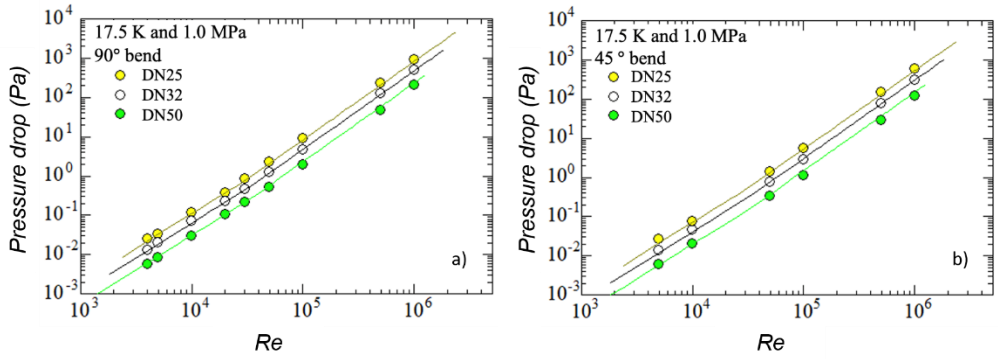


**Figure 6.** Variation of pressure drop with *Re* at **a)** 17.5 K in 90° bend **b)** 17.5 K in 45° bend.

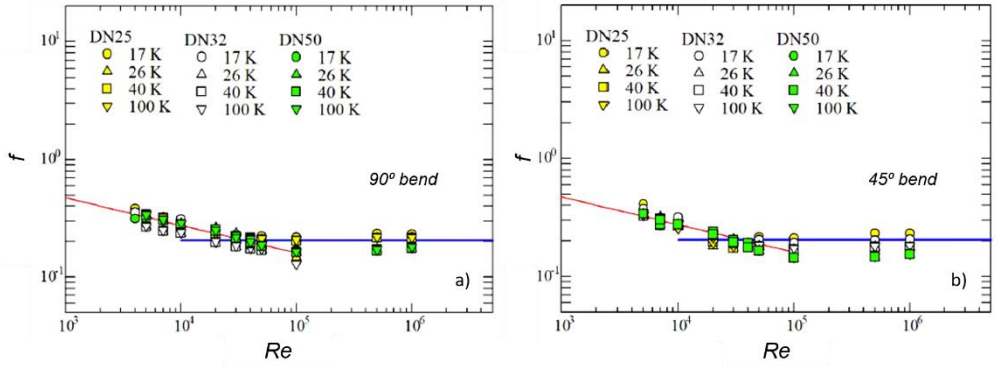


**Figure 7**. Variation of friction factor values in **a)** 90° and **b)** 45° bend, with *Re* at different temperature.

Figure 7 represents the variation of $f$ with *Re* for the 90° and 45° bends at the temperatures ranging from 17.5 K to 100 K. The friction factors appeared to follow a power law with $\alpha = 1$ for $Re < 3.25\times10^4$ almost independent of pipe diameter. For $Re > 3.25\times10^4$, the values of $f$ approached a nearly constant value of 0.211 and 0.20, respectively. It demonstrated that the derived correlation could predict the pressured drops within ±13% errors.

*4.2 Corrugated pipe*

In the CMS, corrugated pipes are used to prevent unexpected stress and damage caused by thermal shrinkage. To derive a pressure drop correlation across the corrugated pipe, 1 m-long such pipe with straight pipe sections with a length of 3.5m and diameters of 25.5 mm, 34.2 mm and 50.4 mm at inlet and outlet was used. The pressure distributions were simulated under the conditions where liquid and gaseous hydrogen flowed at temperatures ranging from 17.5 K to 100 K and a pressure of 1.0 MPa, with *Re* ranging from $5 \times 10^3$ to $1 \times 10^6$. The pressure drops for the corrugated pipes were estimated using the same methodology as that applied to the bends. It was observed that the pressure drop with *Re* followed a power-law relationship for all pipe sizes and decreased with increase in pipe diameter as shown in figure 8(a). A friction factor ($f$) correlation for these pipes has been reported in [4]. In this study, the existing correlation was modified by introducing a correction factor ($\beta$) specific to each pipe size as follows:

$$f = \beta \frac{D_H}{s} \left\{ 1 - \left( \frac{D_H}{D_H + 0.438s} \right)^2 \right\}^2 \quad (3)$$

(For DN25 - $\beta$=0.4115, DN32 - $\beta$=0.5131 & DN5 - $\beta$=0.5573)

where $D_H$ is the hydraulic diameter, and $s$ is the corrugated pitch.

The friction factor for the corrugated pipe calculated using the equation (3) apparently remain almost constant with a value of 0.041, 0.0485 and 0.057 for above stated pipe sizes respectively with some variability around $Re = 5 \times 10^4$. The accuracy of correlation is +/-13%, -20% and -25% for DN25, DN32 and DN50, respectively.

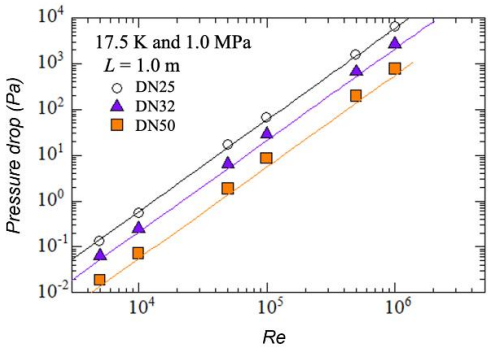


**Figure 8.** Variation of pressure drop in the corrugated pipe with *Re*.

*4.3 Pipe reducer, heat exchanger and moderator*

Figure 9(a) shows the variation in pressure drop across a pipe reducer from *D*=56.3 mm to 38.4 mm as a function of *Re* at temperatures ranging from 17.5 K to 100 K and a pressure of 1.0 MPa. The pressure drop increased with *Re*, following a power-law relationship. The pressure drops initially decreased as the temperature increased from 17.5 K to 40 K. However, with further temperature increase, they increased to values higher than those observed at 17.5 K. This behavior can be attributed to the fact that, for liquids, viscosity decreases with increasing temperature, resulting in lower velocity at the same Reynolds number and consequently a reduced pressure drop. In contrast, for gases, viscosity increases with temperature, leading to higher pressure drops.

Tatsumoto et al. [5] reported that pressure drop through complicated geometries can be represented by introducing a geometric factor ($F$) as follows:

$$\Delta P = F\frac{m^2}{\rho} \tag{4}$$

Figure 9(b) shows the geometric factor for the pipe reducer. The geometric factors became constant across the entire *Re* ranges from $5\times 10^3$ to $1\times 10^6$, regardless of temperature. The correlation can express the pressure drop across the reducer within +5% and -6.5% error.

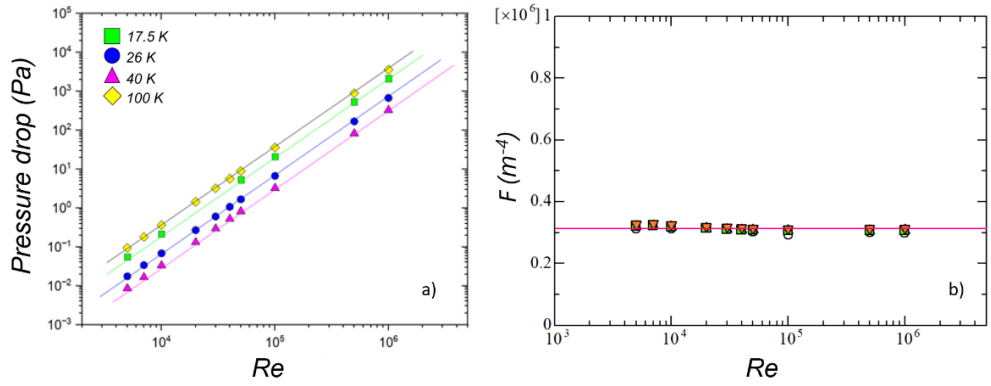


**Figure 9.** Variation of **a)** pressure drop and **b)** geometric factor- *F* with *Re* in a reducer (DN50 to DN32)

Figure 10(a) shows the variation in pressure drop across the heat exchanger as a function of *Re* at temperatures ranging from 17.5 K to 100 K and a pressure of 1.0 MPa. The pressure drop

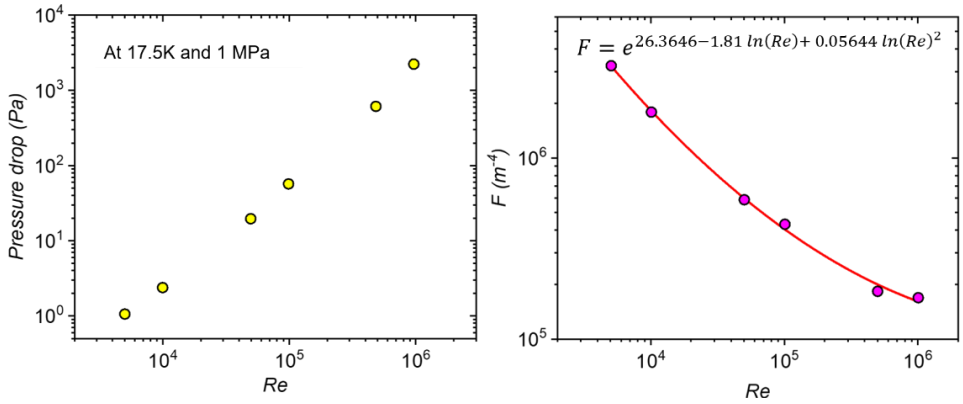


**Figure 10.** Variation of **a)** Pressure drop and **b)** Geometry factor *F* of the Heat Exchanger with *Re*.

increased with *Re*, following a power-law relationship. However, unlike the pipe reducer case, the geometric factor for the heat exchanger decreased with increasing *Re* and appeared to approach a constant value at higher *Re* as shown in Figure 10(b). This trend is likely due to the lower *Re* in the cooling paths of the heat exchanger compared to that in the straight pipe. A fitting curve was derived to estimate the geometric factor as shown in Figure 10(b). This correlation predicts the values within +/-10% error. However, it has been observed that the simulation results are smaller than the measured data from commissioning [6].

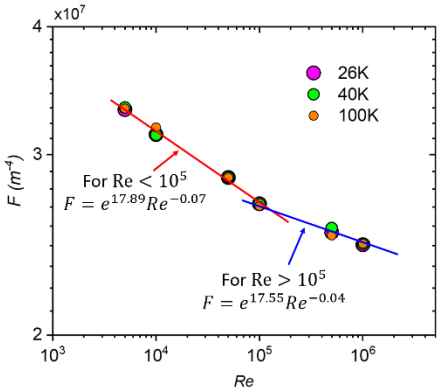


**Figure 11.** Variation of geometric factor-*F* for the Moderator

Pressure drop across a butterfly-shaped moderator was simulated under similar flow conditions. Figure 11 shows the variation of geometric factor for the moderator. Similar to HX, the geometric factors were independent of temperature. Two different correlations were obtained for $Re < 10^5$ and $Re > 10^5$ with prediction error of 1% and 0.5% respectively as shown in Figure 11.

## 5. Estimation of pressure drop in the hydrogen-circulation system

Based on the simulation results, pressure drop correlations were derived as described in Section 4. The pressure drop across each component was then estimated for Helium using the derived correlations under the same condition as those applied during the preliminary CMS commissioning (17.5 K and 0.6 MPa) for validation of work, which was conducted bypassing the moderators using helium. The pressure drops through the valves were calculated by using the flow coefficient of the valve, $K_v$. The total pressure drop was estimated by summation of the individual drops across all CMS components.

Figure 12 shows the calculated pressure drop using the developed correlations across the entire CMS loop, compared with the measured values obtained during the commissioning. As the flow rate increased, the pressure drop increased proportional to $\dot{m}^2$. The predicted pressure drop is 49.5 kPa at mass flow rate of 0.32 g/s, while the measured value obtained during commissioning was 56.3 kPa. The correlations derived in this study predicted the measured pressure drops with an error of ≤13 %. The reasons for this deviation will be analyzed and appropriate actions will be taken to increase the accuracy of the prediction.

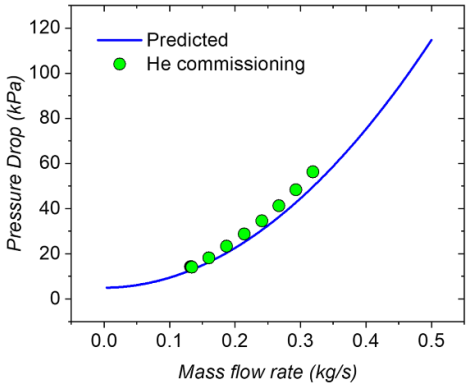


**Figure 12.** Comparison of He commissioning pressure drop and Predicted pressure drop in CMS.

## 6. Conclusion

The pressure drop across each component in the CMS of ESS was estimated over its operational ranges by CFD analysis with ANSYS FLUENT. Pressure drop correlations for each component were formulated based on the simulation results. It was confirmed that the pressure drops measured during the preliminary CMS commissioning with helium aligned with the predicted values from the derived correlation within 13% under the same conditions. The pressure drop predicted by the code for subcooled hydrogen is 41.57 kPa and 165.3 kPa at 17.5 K and 1.0 MPa for mass flow rates of 0.5 kg/s and 1.0 kg/s, respectively.

## References

[1] Garoby R and Danared H et al 2018 Phys. Scr. **93** 014001
[2] H Tatsumoto et al 2024 IOP Conf. Ser.: Mater. Sci. Eng. **1301** 012131
[3] H Tatsumoto et al 2019 IOP Conf. Ser.: Mater. Sci. Eng. **755** 012101
[4] Kanro Duct no Ryutaiteiko 1979 (The Japan Society of Mechanical Engineers) p.33. (in Japanese)
[5] H Tatsumoto et al 2015 IOP Conf. Ser.: Mater. Sci. Eng. **101** 012109
[6] H Tatsumoto et al 2025 ICMC/CEC 2025 Conference. May 2025. Reno, USA.